

Visualisierung der Fahrzeuganströmung für unterschiedliche Karosserievarianten mittels robotischer, volumetrischer LPT.

Flow visualization of the oncoming flow for different vehicle bodies using robotic volumetric LPT.

Timo Gericke, Juan Camilo Londono Alfaro, Steffen Hüttig
Volkswagen AG, Wolfsburg

Karosserie, Shake-The-Box, Lagrangian Particle Tracking, Roboter
Vehicle body, Shake-The-Box, Lagrangian Particle Tracking, Roboter

Abstract

Volumetric flow field measurements are obtained to determine the time-averaged properties of the oncoming flow for different vehicle bodies in an automotive wind tunnel. Measurements are performed with the MiniShaker Aero consisting of a robotic arm and a coaxial volumetric velocimeter (CVV). As tracer particles helium-filled soap bubbles (HFSB) are used. Lagrangian Particle Tracking (LPT) data is analyzed with the Shake-The-Box (STB) algorithm. The two different vehicle bodies are a Sport Utility Vehicle (SUV) and an estate car. Flow fields were measured at a freestream velocity of 50 m/s (SUV) and 44,44 m/s (estate car) giving a Reynolds number based on the car length of $Re_L = 15 \times 10^6$ and $Re_L = 14.5 \times 10^6$, respectively. In total the CVV recorded 36 sub-volumes giving a measurement volume of about $500 \times 500 \times 700 \text{ mm}^3$ (0.294 m^3) upstream of the vehicle bodies. The results show that stagnations regions differ from each other and therefore the velocity distribution.

Introduction

Reducing drag and acoustic noise are two of the main goals of the automotive industry. A deeper understanding of the dominant flow structures is therefore essential to validate numerical simulations on the one hand and to deepen the understanding of the flow physics on the other hand. Here, robotic volumetric LPT-measurements are a useful tool to investigate the flow field of such complex bodies like side mirrors compared to planar two-component, stereoscopic and tomographic PIV.

Large-Scale LPT-measurements around complex objects require the superposition of a multitude of observation domains (sub-volumes) from different perspectives (Jux et al. 2018). This can only be achieved by a measurement system controlled by means of a robotic arm that does not require calibration after repositioning of the system. Schneiders et al. (2018) introduced a compact coaxial volumetric velocimeter (CVV) also called MiniShaker (LaVision GmbH). The MiniShaker Aero MP is a multi-camera system with four cameras and laser expanding optics ideal for Shake-The-Box, double-pulse volumetric PTV and tomographic PIV. Shake-The-Box (Schanz et al. 2016) reduces the computational time compared to conventional tomographic PIV by orders of magnitude (factor of 5-8).

Helium-filled soap bubbles enable PIV/PTV measurements in large air volumes. Due to their size of about 300 μm in diameter the scattering intensity of HFSB is about 10,000 times higher than that of aerosol. Therefore, much larger volumes can be measured or less laser light is necessary. HFSB tracers are neutrally buoyant with a response time of 0.01 ms (Faleiros et al. 2019).

This study describes the robotic volumetric LPT measurements in the wind tunnel facility at Volkswagen AG. The implementation of the measurement system and the measurement procedure as well as parameters indicating the quality of the measurement like dynamic velocity range (DVR) and dynamic spatial range (DSR) are presented. Finally, the 3D flow field upstream of two different vehicle bodies is presented including the main physical properties.

Experimental Setup

Measurements were conducted at the closed loop wind tunnel facility of Volkswagen AG. The atmospheric wind tunnel has an nozzle exit section of 24 m^2 . A maximum wind speed of 55 m/s is possible. In total five linear nozzle arrays (LNA) were placed 1 m downstream of the rain rake. LNA's were attached to the rain simulation rake (dimensions (W x H): 2100 mm x 650 mm) installed during the measurements. Vehicles were placed 4 m downstream of the rain simulation rake. In the investigated setup the LNA, upstream of the car, lead to an increase of the turbulence intensity. Jux et al. (2018) measured a triplication of the turbulence intensity 2 m downstream of a streamlined setup consisting out of four LNAs. Nevertheless, they observed that the seeding rake does not affect the mean velocity by a measurable extend. In the presented setup the rain simulation rake will introduce a much higher turbulence intensity compared to the LNA's. During the measurements, the wind speed was held constant at 50 m/s (SUV) and 44.44 m/s (estate car). Removable paint (Plasti Dip) was used to paint the whole front of the car black in order to reduce reflections of the laser light, thus optimizing the SNR.

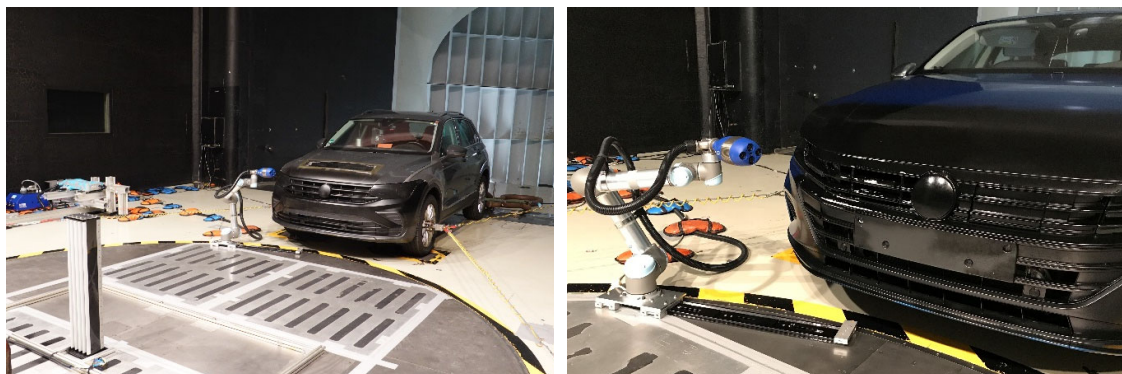


Fig. 1: SUV (left), and estate car (right).

For the acquisitions of the recordings the CVV probe MiniShaker Aero MP (Fig. 1) from La-Vision was used. It exhibits four CMOS-Cameras with a frame rate of 100 Hz at full resolution of 1920 x 1280 pixels with macro planar lenses (f-number = 4, $f\# = 8$ mm) and a pixel pitch Δpx of 4.8 μm . The focal point of the cameras was set at 440 mm from the center of the front cap. In addition, the CVV incorporates a spherical lens for the volumetric laser beam expansion.

Illumination is provided by a Litron NanoPIV Nd:YAG laser with an output energy of 50 mJ per pulse at a wavelength of 532 nm and a frequency of 100 Hz. Laser light was transmitted with

an optical fiber towards the CVV's head. The measurable volume, is bound within the region where the camera views overlap in lateral and vertical direction. At a measurement distance of $z = 260$ mm, the FOV attains 220×130 mm² which extends to 450×350 mm² at $z = 670$ mm. Synchronization between the laser and the cameras was assured by a PTU X from LaVision. The CVV heads position and orientation is controlled by a robotic arm UR5 from Universal Robots (Jux et al. 2018) with six degrees of freedom (3 rotation and 3 translation axes), similar to the movement range of a human arm. Position repeatability is stated by the manufacturer as ± 0.1 mm (Universal Robots). Maximum reach of the UR5 stretches 850 mm in radius around the robot base.

Helium-filled soap bubbles were used as tracer particles with a mean size of 300 μ m. A HFSB generator from LaVision was used to generate the seeding particles. The system consists of a fluid supply unit (FSU), one base profile, five linear nozzle arrays (LNAs) and a power supply unit (included in FSU). Span width of the LNA is 874.5 mm with a profile chord of 186.6 mm and a profile thickness of 29.9 mm. In total 20 nozzles are distributed over the span width of the LNA. Each nozzle produces up to 40.000 soap bubbles per second. In total $\sim 4 \times 10^6$ tracers per second are produced, distributed over a cross section of 200×874.5 mm².

A single-plane calibration plate (LaVision Type 286-39 SSSP), mounted to optomechanical components, is used for the geometric calibration. The calibration plate consists of 42 dots with a center-to-center spacing of 40 mm and a dot diameter of 12 mm. Geometrical calibration was performed with five different views at $z = 440$ mm and the pinhole method. After the geometric calibration a volume self-calibration (Wieneke 2008) followed by the determination of the optical-transfer-function (OTF) (Schanz et al. 2012) is performed with the use of experimental data in DaVis 10.2.

For particle image recording the robot base was placed 1135 mm away from the car centerline. Measurements are gathered from a total of 36 positions. At each position 1000 double-frame images are recorded at a recording rate of 50 Hz.

Raw particle images are pre-processed using the image pre-processing routine in DaVis 10.2. Main goal of the pre-processing is the removal of background noise from the image in order to have clearly defined particle images with high contrast between the particles and the background. After the image pre-processing the particle images were analyzed with the Shake-The-Box algorithm implemented in DaVis. Every sub-volume contains approximately 600.000 tracks (600 per image pair). After the particles are tracked, the sub-volumes were merged together (Stitching). Afterwards the Lagrangian description of the velocity was converted into a Eulerian description through the binning process. The result is the mean velocity vector field. The interrogation window's size is 128 voxel with 75% overlap resulting in a grid size of 32 voxel (5.4 mm).

The dynamic spatial range DSR is defined as the ratio between the largest and the smallest measurable length scales (Adrian 1997). For the present setup the largest length scale is given by the length of the measured sub volumes and the smallest length scale is given by the smallest used bin size.

$$\overline{DSR} = \frac{450 \text{ mm}}{5.4 \text{ mm}} = 83 \quad (1)$$

Another important parameter is the dynamic velocity range (DVR). The DVR is defined as the ratio between the maximum resolvable velocity and the minimum one (Adrian 1997). In the present case the ratio between the maximum measured velocity and the measurement uncertainty in the overlapping region of adjacent sub volumes.

$$\overline{DVR} = \frac{28 \text{ m/s}}{0.2 \text{ m/s}} = 140 \quad (2)$$

Results

The PTV results for the two different vehicle bodies (SUV & estate car) are presented in Fig. 2 at two different y/L positions, normalized with the mean freestream velocity for both measurements. Clearly visible are the two stagnation regions for both vehicle bodies in the centerline at $y/L = 0$. It can also be seen that only a stagnation region for the SUV is there at the outer centerline position $y/L = 0.08$ (0.07). This is a clear effect of the much bigger stagnation region in the case of the SUV. Moreover, due to the smaller stagnation regions in the case of the estate car higher velocities were measured especially in the upper half of the FOV.

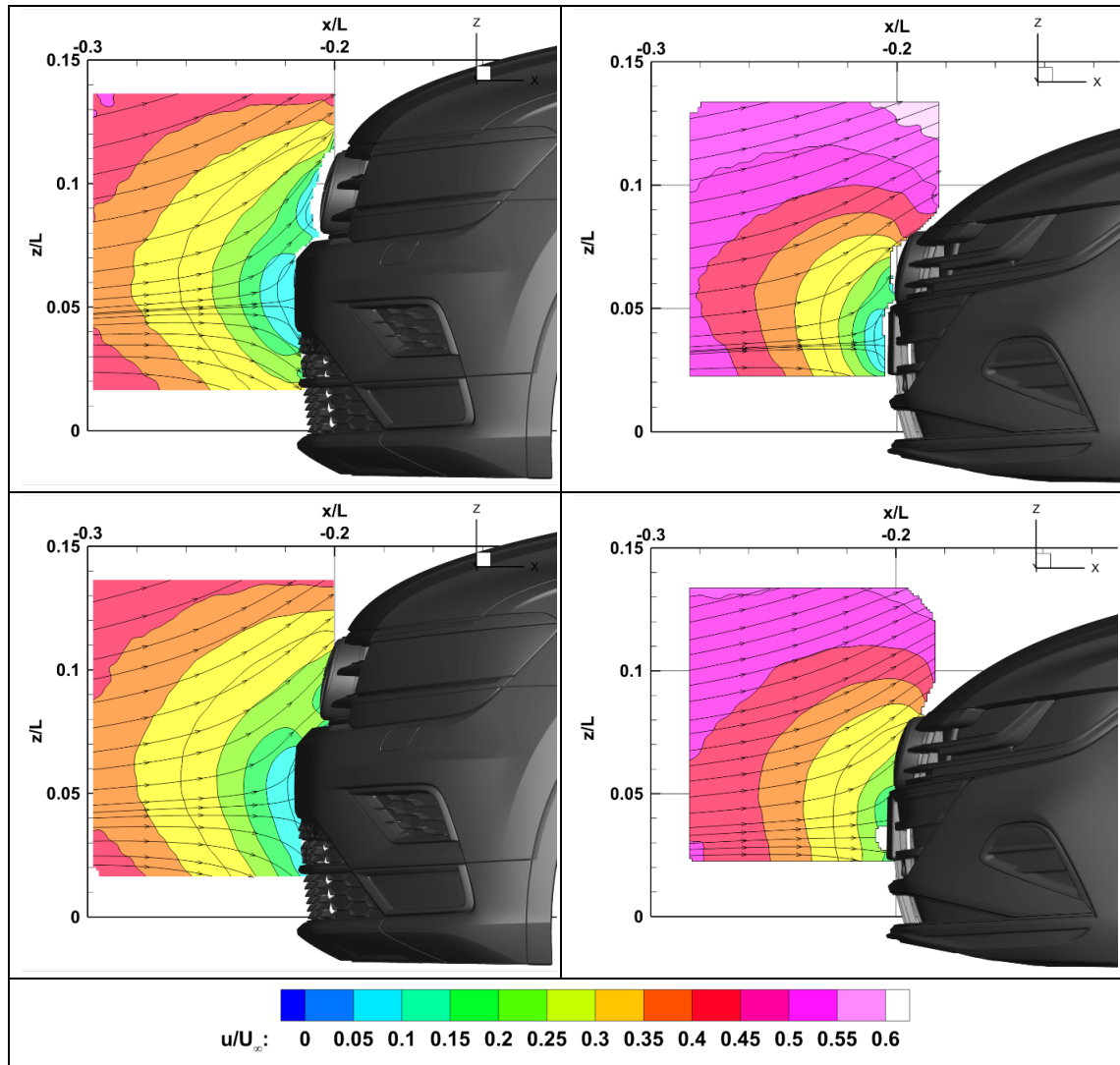


Fig. 2: Contour map of the averaged velocity u/U_∞ in the y - z plane at $y/L = 0$ (top) and at $y/L = 0.08$ & 0.07 (bottom). SUV at $Re_L = 15 \times 10^6$ (left) and estate car at $Re_L = 14.5 \times 10^6$ (right).

In Fig. 3 the results of the mean velocity field for $Re_L = 15 \times 10^6$ and $Re_L = 14.5 \times 10^6$ visualized by five perpendicular vector planes is shown. Here, the dimensions of the stagnations areas and the different velocity distributions become much clearer. It should be noted that in none of the measurements the freestream velocity of one or even higher is reached. This can be expected from literature (e.g. Varney et al. 2020) at positions greater than $x/l = -0.2$ on top of the hood.

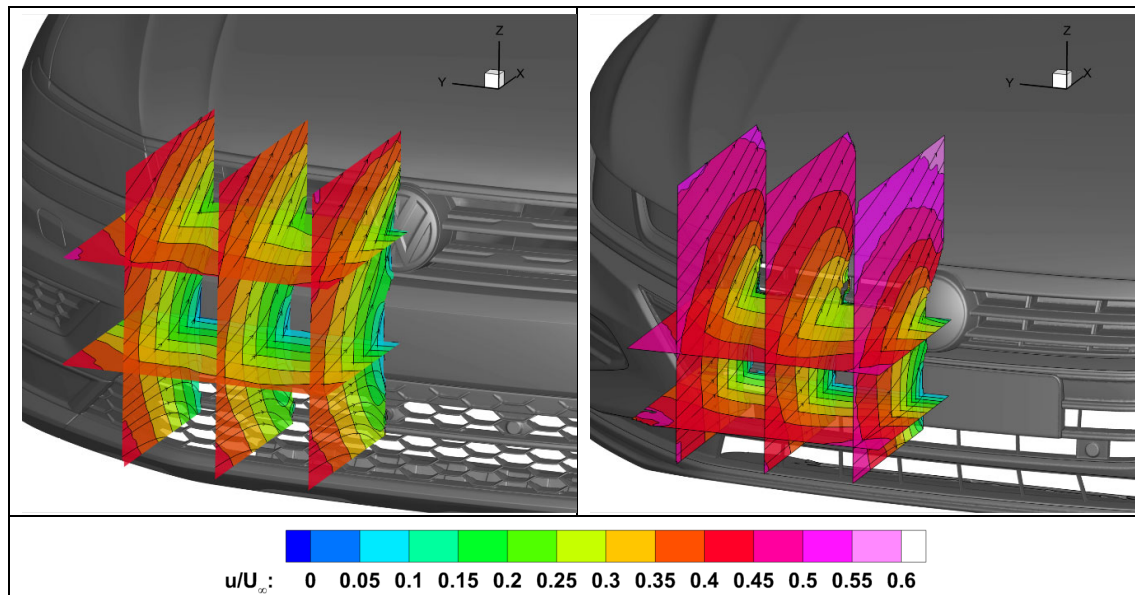


Fig. 3: Result of 3D mean velocity field for $Re_L = 15 \times 10^6$ (left) and $Re_L = 14.5 \times 10^6$ (right) based on bin-averaging approach and visualized by five perpendicular vector planes color coded by the stream-wise velocity.

The reason for this is the during the measurements installed rain simulation rake which leads to an first displacement of the flow four meters before the car.

Conclusion

This paper presents volumetric LPT measurements of the oncoming flow for two different vehicle bodies (SUV & estate car) at different Reynolds numbers ($Re_L = 15 \times 10^6$ and $Re_L = 14.5 \times 10^6$) in a closed loop wind tunnel with a nozzle exit diameter of 24 m².

For the SUV the stagnation area is much bigger compared to the estate car. Hence velocities for the estate car in the measured volume are higher.

The results, opinions and conclusions expressed in this publication are not necessarily those of Volkswagen Aktiengesellschaft.

Acknowledgment

The authors would like to acknowledge the colleagues from LaVision for their support throughout the measurement campaign and the evaluation phase.

Literature

Adrian, R. J. 1997: "Dynamic ranges of velocity and spatial resolution of particle Image velocimetry", Meas Sci Technol, 8(12):1393

Faleiros, D.E., tuinstra, M., Sciacchitano, A., Scarano, F., 2019: "Generation and control of helium-filled soap bubbles for PIV", Exp. Fluids 60(3): 40

Jux, C., Sciacchitano, A.; Schneiders, J.F., Scarano, F., 2018: "Robotic volumetric PIV of a full-scale cyclist", Exp. Fluids 59(4): 74

Schanz, D., Gesemann, S., Schröder, A., Wieneke, B., Novara, M., 2012: "Non-uniform optical transfer functions in particle imaging: calibration and application to tomographic reconstruction", Meas Sci Technol, 24: 024009

Schanz, D., Gesemann, S., Schröder, A., 2016: "Shake-The-Box: Lagrangian particle tracking at high particle image densities", Exp. Fluids 57(5): 70

Schneiders, J.F.G., Jux, C., Sciacchitano, A.; Scarano, F., 2018: "Coaxial volumetric velocimetry", Meas. Sci. Technol. 29: 065201

Varney, M.; Passmore, M., Wittmeier, F., Kuthada, T., 2020: "Experimental Data for the Validation of Numerical Methods: DrivAer Model", Fluids 5, 236

Wieneke, B., 2008: "Volume self-calibration for 3D particle image velocimetry", Exp. Fluids, 45(4): 549–556